Spin-glass-like behaviour and low-temperature specific heat of amorphous Er_xNi_{100-x} random magnetic anisotropy system

1995 J. Phys.: Condens. Matter 7 4193

(http://iopscience.iop.org/0953-8984/7/22/003)

J. Phys.: Condens. Matter 7 (1995) 4193–4205. Printed in the UK

Spin-glass-like behaviour and low-temperature specific heat of amorphous Er_xNi_{100-x} random magnetic anisotropy system

Y Hattori†, K Fukamichi†, K Suzuki‡, H Aruga-Katori§ and T Goto§

† Department of Materials Science, Faculty of Engineering, Tohoku University, Sendai 980-77, Japan

‡ Institute for Materials Research, Tohoku University, Sendai 980-77, Japan

§ Institute for Solid State Physics, The University of Tokyo, Roppongi, Minato-ku, Tokyo 106, Japan

Received 12 September 1994, in final form 28 February 1995

Abstract. Spin-glass-like behaviour and low-temperature specific heat have been investigated for bulk amorphous Er_xN_{100-x} ($x = 33, 50$ and 80) alloys prepared by high-rate direct-current sputtering. The competition between ferromagnetic and antiferromagnetic interactions arising from the exchange fluctuations is negligibly small in this system, in contrast to that in amorphous Er–Cu alloys. The random magnetic anisotropy (RMA) suppresses the ferromagnetic coupling, resulting in a spin-glass-like state. The magnetization per Er atom becomes smaller with increasing Er content owing to the increase in the RMA.

At the spin freezing temperature T_f, the low-temperature specific heat exhibits a broad maximum, which becomes narrower with the decrease in Er content. It should be noted that the temperature at which the magnetic specific heat of the amorphous $Er_{33}Ni_{67}$ alloy reaches a maximum value coincides with the T_f determined by the alternating-current magnetic susceptibility measurement. The splitting of the ground state from $J = 15/2$ into a Kramers doublet is caused by the electrostatic field, being accompanied by a Schottky-type specific heat with a linear temperature dependence. The magnetic entropy at T_f is estimated to be about 45–60% of the theoretical value, being much larger than those for crystalline dilute spin-glass systems. Moreover, the plot of the magnetic specific heat versus $T^{3/2}$ is linear at low temperatures. Therefore, it is considered that a ferromagnetic-like spin wave is excited, although its magnetic structure is not ferromagnetic.

1. Introduction

In the last two decades, a great number of magnetic properties for amorphous alloys containing non-S-state rare-earth (RE) elements have been investigated (Harris *et al* 1973, Coey 1978, Filippi *et al* 1985, O'Shea and Lee 1991). In these amorphous alloys, the local electrostatic field acts on the 4f moment of the RE element and produces a large anisotropy randomly oriented owing to the random atomic arrangement. The magnetic properties of these alloys are strongly affected by this anisotropy, called the random magnetic anisotropy (RMA) (Harris *et al* 1973). Theoretical (Aharony and Pytte 1980) and experimental (Boucher 1977a, Coey *et al* 1981) studies have revealed that the RMA brings about a spin-glass-like state. That is, the RMA suppresses the ferromagnetic coupling of the RE moment, resulting in a speromagnetic structure.

The competition of ferromagnetic and antiferromagnetic interactions due to the exchange fluctuations also causes a spin-glass state as in crystalline magnetically dilute AuFe (Cannella and Mydosh 1972) and CuMn (Coles *et al* 1978) alloys and amorphous Gd-based alloys

0953-8984/95/224193+13$19.50

(Mizoguchi *et al* 1977). It is, therefore, interesting to investigate the physical properties of the RMA systems and to compare them with those of spin-glass systems from the viewpoint of the different origin of spin freezing. The competition of ferromagnetic and antiferromagnetic interactions arising from the existence of the exchange fluctuations has been pointed out even in amorphous non-S-state RE alloys (Sellmyer and Nafis 1985). In fact, the magnetic properties of the amorphous RE–Cu alloys are affected by both random magnetic anisotropy and fluctuations of the exchange interactions (Hattori *et al* 1995). In contrast to the amorphous RE–Cu alloys, the RMA dominantly governs the magnetic properties of amorphous RE–Ni alloys because the competition of exchange interactions is very small, as given in the discussion. Further, Ni is regarded to be non-magnetic in amorphous Er_xNi_{100-x} ($x \geqslant 33$) alloys because the magnetic moment of the Ni vanishes in amorphous $Dy_{25}Ni_{75}$ (Rebouillat *et al* 1977) and Y_xNi_{100-x} ($x \geqslant 17$–22) alloys (Liénard and Rebouillat 1978, Beille *et al* 1979, Gignoux *et al* 1982, Fujita *et al* 1993). Therefore, the investigation of amorphous non-S-state RE–Ni alloys sheds light on the effect of the RMA on the magnetic properties.

From the viewpoint of phase transition, many researchers have paid much attention to the specific heat in the vicinity of the spin freezing temperature T_f for spin-glass systems (Wenger and Keesom 1976, Meschede *et al* 1980, Miyako *et al* 1979). In spin-glass systems such as crystalline magnetically dilute CuMn alloys and $Eu_xSr_{1-x}S$ compounds, the maximum temperature of the magnetic contribution to the specific heat does not coincide with T_f (Wenger and Keesom 1976, Meschede *et al* 1980). In Er-based alloys, the magnetic ordering temperature is low owing to the small de Gennes factor. The evaluation of magnetic entropy becomes accurate because the lattice specific heat, which should be subtracted, rapidly decreases with temperature. Therefore, the amorphous Er–Ni alloy system is appropriate to investigate the influence of the RMA on the low-temperature specific heat. In the present study, therefore, the magnetic properties and the low-temperature specific heat have been investigated for amorphous Er_xNi_{100-x} alloys.

2. Experimental details

Alloy targets were made by arc-melting 99.9 wt.% pure Er, Y and Ni in an argon atmosphere purified with a Ti getter. For easy measurements, bulk amorphous Er_xNi_{100-x} ($x = 33, 50$ and 80) and $Y_{33}Ni_{67}$ alloys of about 0.2–0.3 mm thickness were prepared by a high-rate DC triode sputtering for three days on a water-cooled Cu substrate. The Cu substrate was removed from the samples by mechanical polishing. Their amorphous state was confirmed by x-ray diffraction using Cu Kα radiation. The magnetization up to 55 kOe and the magnetic field cooling effect were measured with a SQUID magnetometer (Quantum Design, MPMS). Very high-field magnetization measurements up to 360 kOe were carried out with a pulse magnet. The AC magnetic susceptibility was measured by a mutual induction method at 80 Hz in an AC magnetic field of 1 Oe. The low-temperature specific heat was measured from 1.8 to 15 K by a heat-pulse method, cooling being achieved by a helium bath at 1 K via a mechanical heat switch. The bulk sample with a mass of about 0.5 g was fixed with nylon lines in a chamber evacuated to about 10^{-7} Torr to keep the thermal isolation.

3. Results and discussion

Figure 1 shows the temperature dependence of the DC magnetic susceptibility and its inverse susceptibility for amorphous Er_xNi_{100-x} ($x = 33, 50$ and 80) alloys from 4 to 300 K in a

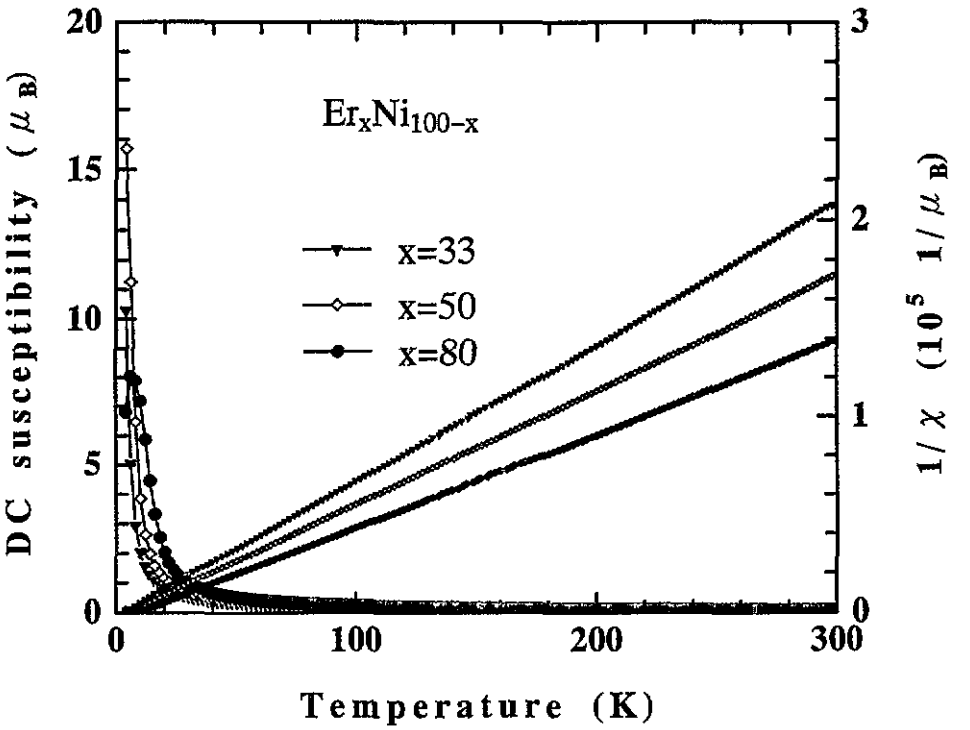

Figure 1. Temperature dependence of the DC magnetic susceptibility and its inverse susceptibility for amorphous Er_xENi_{100-x} ($x = 33, 50$ and 80) alloys.

field of 1 kOe. In wide temperature ranges, they exhibit a Curie–Weiss type of temperature dependence with effective magnetic moment $P_{eff} = 9.7$–$10.0\ \mu_B$, close to that of free Er^{3+} ion. The paramagnetic Curie temperature θ_p is positive, indicating that the Er–Er exchange interaction is dominantly ferromagnetic. The values of θ_p for $x = 33, 50$ and 80 are 4.4, 5.7 and 9.8 K, respectively. The magnetic susceptibility deviates from the Curie–Weiss law at very low temperatures, suggesting the existence of some magnetic ordering. The magnetic field cooling effect has been measured in order to confirm the magnetic ordering. Shown in figure 2 is the temperature dependence of zero-field cooled (ZFC) and field cooled (FC) magnetizations for the amorphous $Er_{80}Ni_{20}$ alloy measured in various magnetic fields. A clear hysteresis between ZFC and FC magnetizations is observed. The temperature of the onset of hysteresis corresponds to the temperature at which the ZFC magnetization reaches a maximum value, and it decreases with increasing magnetic field. Other different compositional alloys show a similar magnetic field cooling effect. Moreover, the AC susceptibility of the amorphous Er_xNi_{100-x} ($x = 33, 50$ and 80) alloys exhibits the characteristic cusp of a spin glass as seen in figure 3. Therefore, it is clear that the amorphous Er_xNi_{100-x} alloys exhibit spin-glass-like behaviour. Figure 4 shows the concentration dependence of the spin freezing temperature T_f. With increasing Er content, T_f increases in a similar manner to θ_p. Shown in figure 5 is the field dependence of T_f in a DC magnetic field up to 500 Oe for the amorphous $Er_{80}Ni_{20}$ alloy, together with the data obtained by the AC susceptibility measured in 1 Oe. The freezing temperature T_f is determined from the onset of irreversibility between ZFC and FC magnetizations. With the increase in the magnitude of magnetic field, T_f decreases as seen from the figure. The $H^{2/3}$

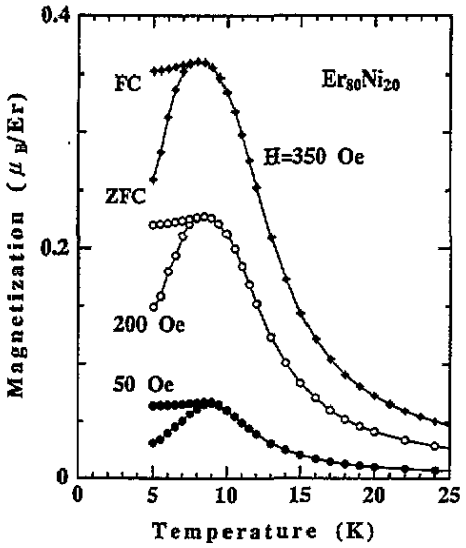

Figure 2. Temperature dependence of zero-field cooled (ZFC) and field cooled (FC) magnetizations for the amorphous $Er_{80}Ni_{20}$ alloy as a function of the mangetic field.

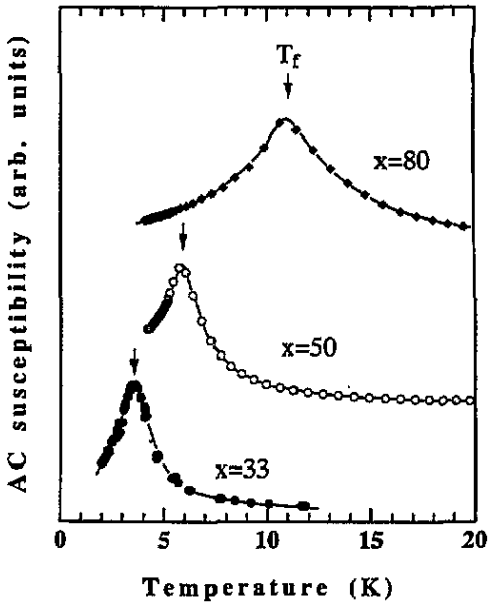

Figure 3. Temperature dependence of the AC magnetic susceptibility for the amorphous Er_xNi_{100-x} (x = 33, 50 and 80) alloys at 80 Hz in a field of 1 Oe.

dependence of T_f is not observed, implying that it does not follow the Almeida–Thouless law (de Almeida and Thouless 1978) in the present study. Precise measurements in much lower field are necessary for more detailed discussion.

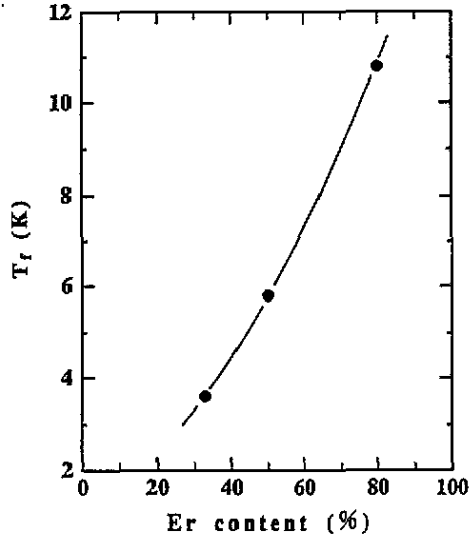

Figure 4. Concentration dependence of the spin freezing temperature T_f for the amorphous Er_xNi_{100-x} (x = 30, 50 and 80) alloys.

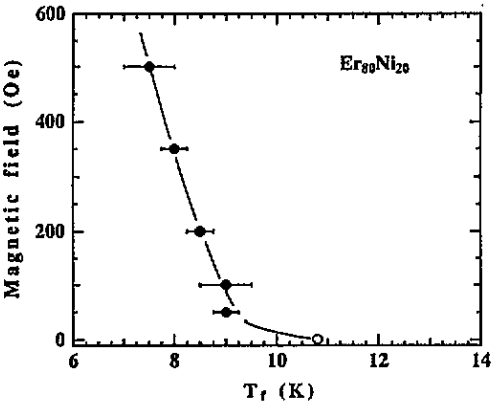

Figure 5. DC magnetic field dependence of the spin freezing temperature T_f for amorphous $Er_{80}Ni_{20}$ alloy (full circle), together with the result obtained at 80 Hz in an AC magnetic field of 1 Oe (open circle).

The spin-glass-like state of the amorphous alloys containing a RE element is caused by the competition of ferromagnetic and antiferromagnetic interactions due to the exchange fluctuations and/or the random magnetic anisotropy (RMA) as mentioned in the introduction. The Hamiltonian has been proposed by taking the fluctuations of exchange interaction into consideration (Sellmyer and Nafis 1985):

$$H = -\sum(J_0 + \Delta J_{ij})S_iS_j - D\sum(n_i \cdot S_i)^2 - g\mu_B H\sum J \tag{1}$$

where J_0 is the average ferromagnetic interaction, ΔJ_{ij} the exchange fluctuations, D the random magnetic anisotropy, n_i the random easy-axis direction, g the Landé g-factor and J the total angular momentum. Experimentally, it has been pointed out that both the RMA and fluctuations of the exchange interaction play an important role in the magnetic properties for amorphous Er_xCu_{100-x} alloys (Hattori *et al* 1995). In this system, the competition between ferromagnetic and antiferromagnetic interactions due to the exchange fluctuations becomes remarkable below about $x = 50$. That is, the paramagnetic Curie temperature θ_p, which reflects the magnitude of the sum of all exchange interactions exhibits a rapid decrease below about $x = 50$ because of the rapid increase in antiferromagnetic Er–Er exchange interactions (Hattori *et al* 1995). To show the negligibly small effect of the exchange fluctuations in amorphous Er–Ni alloys, we consider the exchange interactions in amorphous S-state Gd–Al alloys without the RMA because of no orbital angular momentum.

The concentration dependence of the RKKY interaction for the amorphous Gd_xAl_{100-x} alloys has been discussed using a simple free-electron model (Mizoguchi *et al* 1977, Jamet and Malozemoff 1978). The q value given by the following expression has been estimated by assuming the Gd–Gd nearest-neighbour distance $r_n = 3.6$ Å and the numbers of the conduction electrons $n_0 = 3$:

$$q = 4\pi r_n\left(\frac{3n_0}{8\pi V_a}\right)^{1/3} \tag{2}$$

where the average atomic volume V_a is obtained by a linear interpolation between the atomic volumes V_{Gd} and V_{Al}. From equation (2), the Gd concentration x is given by the following

expression:

$$x = \frac{(3n_0/8\pi)(4\pi r_n/q)^3 - V_{Al}}{(V_{Gd} - V_{Al})}. \tag{3}$$

The q value for amorphous Gd_xAl_{100-x} falls in the range spanning to the second zero of the RKKY oscillation. The distribution of the Gd–Gd distance caused by the random atomic structures in the amorphous state gives rise to the fluctuations of exchange interactions, the possibility of both ferromagnetic and antiferromagnetic interactions. From equation (3), it is clear that the Gd concentration x shifts to a lower q region with increasing n_0. Therefore, it is expected that the competition between ferromagnetic and antiferromagnetic interactions becomes weaker with the increase in n_0 and/or the decrease in V_{Al}. Comparing amorphous Gd_xNi_{100-x} alloys with Gd_xCu_{100-x} alloys, the competition between the ferromagnetic and antiferromagnetic interactions in the former is much smaller than that in the latter because the value of n_0 of Ni and Cu is 2 and 1, respectively, although the atomic volumes of Ni and Cu are close to each other (Hattori *et al* 1995). In fact, it has been reported that an amorphous $Gd_{31}Cu_{69}$ alloy is a spin glass (Mizoguchi *et al* 1977, McGuire *et al* 1978), whereas an amorphous $Gd_{26}Ni_{74}$ alloy is ferromagnetic with $T_c = 38$ K (Asomoza *et al* 1979). The relation given by equation (3) is considered to be valid for amorphous Er-based alloys, although the total angular momentum J is much larger than that in the Gd alloys. That is to say, the magnetic properties of the amorphous Er_xNi_{100-x} ($x = 33, 50$ and 80) alloys are considered to be well described by the following Hamiltonian without the contribution from the exchange fluctuations (Harris *et al* 1973):

$$H = -\sum J S_i S_j - D \sum (n_i \cdot S_i)^2 - g\mu_B H \sum J. \tag{4}$$

Therefore, the amorphous Er_xNi_{100-x} ($x = 33, 50$ and 80) alloy system is appropriate to investigate the effect of the RMA on the magnetic properties.

Figure 6 shows the magnetization per Er atom of the amorphous Er_xNi_{100-x} ($x = 33, 50$ and 80) alloys up to 360 kOe at 4.2 K. The magnetization curves are not saturated easily with a strong curvature because the RMA disturbs the ferromagnetic couplings of Er–Er. The magnitude of magnetization per Er atom decreases with increasing Er content. The random magnetic anisotropy constant D is related to the high-field susceptibility, χ_{hf}, and given by the following expression (Asomoza *et al* 1979):

$$D = \frac{g^2\mu_B^2}{3\chi_{hf}}\left(1 + \frac{3k_B\theta_p\chi_{hf}}{g^2J^2\mu_B^2}\right) \tag{5}$$

where θ_p is the paramagnetic Curie temperature and k_B the Boltzmann constant. The values of D for the amorphous $Er_{33}Ni_{67}$, $Er_{50}Ni_{50}$ and $Er_{80}Ni_{20}$ alloys are 4.9 K, 5.6 K and 7.9 K, respectively, comparable to the results reported previously for amorphous $Er_{25}Ni_{75}$ (Asomoza *et al* 1979), $(RE_{75}Au_{25})_{90}B_{10}$ (RE=Pr, Tb and Er) (Sellmyer *et al* 1980) and Er_xCu_{100-x} ($x = 30, 40, 50$ and 70) (Hattori *et al* 1995) alloys. Thus, the RMA increases with the increase in the Er content. Figure 7 shows the Arrott plots of the amorphous $Er_{80}Ni_{20}$ alloy. The plots deviate from linearity and the finite intercepts with the M^2 axis below T_f are absent, which indicates the lack of finite spontaneous magnetization, consistent with the theoretical prediction concerning the absence of long-range order (Aharony and Pytte 1980).

It has been pointed out that the magnetic contribution to the specific heat shows no marked anomaly at the spin freezing temperature T_f in crystalline spin-glass systems (Wenger

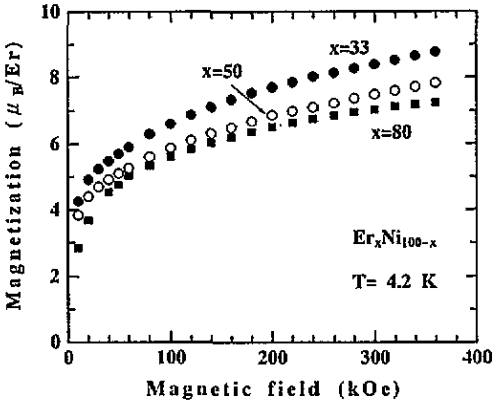

Figure 6. Magnetization per Er atom up to 360 kOe at 4.2 K for the amorphous Er_xNi_{100-x} (x = 33, 50 and 80) alloys.

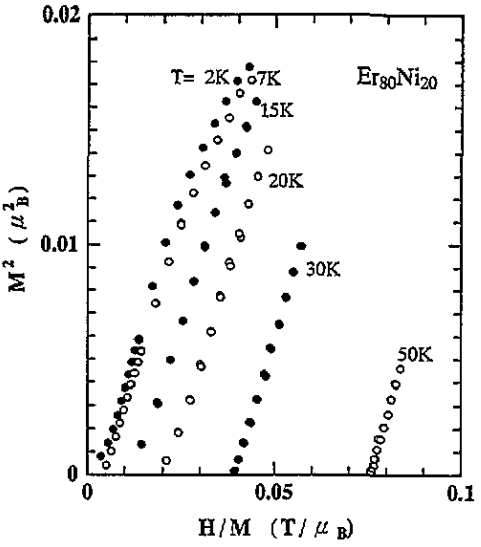

Figure 7. Arrott plots for the amorphous $Er_{80}Ni_{20}$ alloy.

and Keesom 1976, Meschede *et al* 1980). It is interesting to investigate the magnetic specific heat characteristics in RMA systems, because the cause of the spin freezing is not the competition between ferromagnetic and antiferromagnetic interactions but the RMA. Figure 8 shows the temperature dependence of the low-temperature specific heat C_p per mole of Er atoms for amorphous Er_xNi_{100-x} (x = 33, 50 and 80) alloys. The temperature at which the specific heat reaches a maximum value does not coincide with the spin freezing temperature in spin-glass systems such as crystalline magnetically dilute CuMn alloys (Wenger and Keesom 1976) and $Eu_xSr_{1-x}S$ (x = 0.40 and 0.54) compounds (Meschede *et al* 1980). Therefore, the phase transition of the spin glass is considered to be different from those of ferromagnetic and antiferromagnetic long-range magnetic orderings. It is worth noting that the C/T of the spin-glass system $(Ti_{0.99}V_{0.01})_2O_3$ exhibits a maximum at T_f, suggesting a high-order phase transition (Miyako *et al* 1979). As seen in figure 8, C_p of the amorphous Er_xNi_{100-x} (x = 33 and 50) alloys exhibits a broad maximum at T_f determined from the temperature dependence of AC susceptibility. The coincidence of the magnetic specific heat maximum with the magnetic ordering temperature in the present alloys is analagous to that of a long-range magnetic order transition. A broad maximum of the low-temperature specific heat at a temperature about 1.3 K higher than T_f has been reported in an amorphous $Dy_{32}Ni_{68}$ alloy (von Molnar *et al* 1982). However, it should be borne in mind that T_f is very sensitive to the experimental conditions, and the determination of T_f from the thermomagnetization curve in a DC magnetic field of 44.7 Oe is considered to be inadequate. As seen from figure 5, T_f is very sensitive to the applied magnetic field. Therefore, it seems reasonable to assume that the maximum temperature of specific heat also corresponds with T_f for the amorphous $Dy_{32}Ni_{68}$ alloy mentioned above. The specific heat maximum becomes broader with the increase in the Er content and the lattice specific heat becomes larger compared with that of the amorphous $Er_{33}Ni_{67}$ and $Er_{50}Ni_{50}$ alloys, and hence the magnetic specific heat in the vicinity of T_f is vague in the amorphous $Er_{80}Ni_{20}$ alloy, as given in the inset of figure 8.

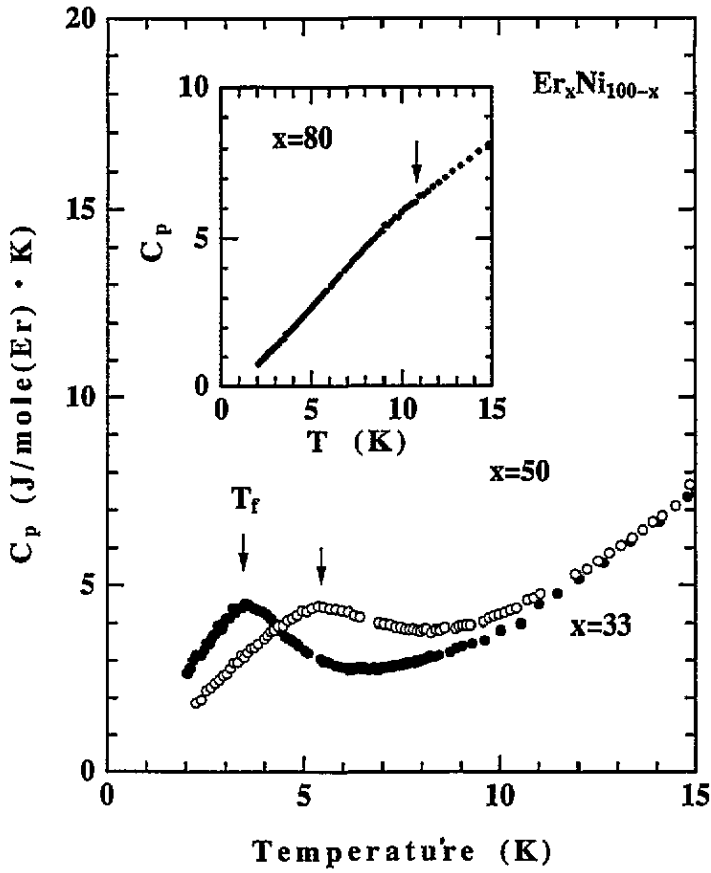

Figure 8. Temperature dependence of the low-temperature specific heat C_p per mole of Er atoms for the amorphous Er_xNi_{100-x} (x = 33, 50 and 80) alloys. The arrows indicate the spin freezing temperature T_f determined from the temperature dependence of the AC magnetic susceptibility.

Figure 9 shows the temperature dependence of low-temperature specific heat in the form of C_p/T versus T^2 for amorphous $Er_{33}Ni_{67}$ and $Er_{50}Ni_{50}$ alloys, together with that of an $Y_{33}Ni_{67}$ alloy, for comparison. The slopes of C_p/T for the amorphous $Er_{33}Ni_{67}$ and $Y_{33}Ni_{67}$ alloys are almost the same and the Debye temperature θ_D is estimated to be 200 K. The value of θ_D for the amorphous $Er_{50}NI_{50}$ alloy is about 180 K. The coefficient of the linear term for the amorphous $Er_{33}NI_{67}$ and $Er_{50}Ni_{50}$ alloys is about 290 and 350 mJ (mol Er)$^{-1}$ K^{-2}, being two orders of magnitude larger than the value of 7 mJ (mol Y)$^{-1}$ K^{-2} for the amorphous $Y_{33}Ni_{67}$ alloy. Such a large linear term has been predicted for RMA systems (Korenblit and Shender 1978) and reported for an amorphous $Dy_{52}Cu_{48}$ alloy (von Molnar *et al* 1982). Assuming the splitting of the ground state of $J = 15/2$ into eight doublets due to the electrostatic field and the constant effective molecular field H_m, the Zeeman energy ε_i at site i will be $\pm g\mu_B H_m^i \cdot S_z^i = A\cos\theta_i$. We consider only the lowest doublet at low temperatures. Therefore, the Schottky-type specific heat is given by the following expression (von Molnar *et al* 1982):

$$C_s = \frac{\partial U}{\partial T} = \frac{\partial}{\partial T}\int d\Omega P(\Omega)\frac{-\varepsilon\exp(\varepsilon/kT) + \varepsilon\exp(-\varepsilon/kT)}{\exp(-\varepsilon/kT) + \exp(\varepsilon/kT)} \tag{6}$$

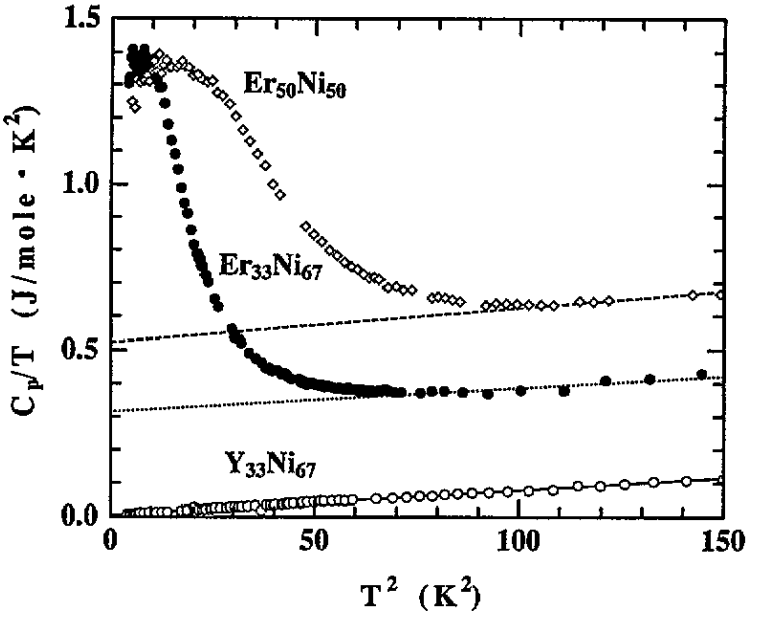

Figure 9. Low-temperature specific heat in the form of C_p/T versus T^2 for amorphous $Er_{33}Ni_{67}$ and $Er_{50}Ni_{50}$ alloys, together with that for amorphous $Y_{33}Ni_{67}$ alloy.

with $d\Omega = \sin\theta\, d\theta\, d\phi$, where $P(\Omega)$ is the probability of finding any solid angle, Ω. In a complete random system, $P(\Omega) = 1$, and hence one can find

$$C_s = \frac{\pi^2 N k_B^2}{12 g \mu_B H_m S_z} T = \delta T. \tag{7}$$

The linearity of the C/T versus T^2 plot for amorphous $Er_{33}Ni_{67}$ and $Er_{50}Ni_{50}$ alloys implies the Schottky-type contribution of the linear term to the specific heat. Therefore, the large linear term of the specific heat does not come from the large value of the electronic density of states at the Fermi level, as in heavy-fermion systems, but from the Schottky-type specific heat. The linear temperature dependence directly indicates that the anisotropy axes are not correlated, i.e. they are random as pointed out previously (von Molnar *et al* 1982). Taking the Schottky-type specific heat C_s into consideration, the magnetic specific heat C_{mag} of the RMA system is given as

$$C_{mag} = C_{total} - (\gamma T + \alpha T^3 + C_s) = C_{total} - (\gamma T + \alpha T^3 + \delta T) \tag{8}$$

where γ and α are electronic and lattice specific heat coefficients, respectively. The value of θ_D for the amorphous $Er_{33}Ni_{67}$ alloy is almost the same as that of the amorphous $Y_{33}Ni_{67}$ alloy. Shown in figure 10 is the temperature dependence of the magnetic contribution to the specific heat and the AC susceptibility of the amorphous $Er_{33}Ni_{67}$ alloy. The maximum temperature of the magnetic specific heat coincides with T_f determined by the AC magnetic susceptibility measurement, which is different from the data for the crystalline magnetically dilute alloy systems mentioned before. This difference would come from the distinction of the origin of spin freezing.

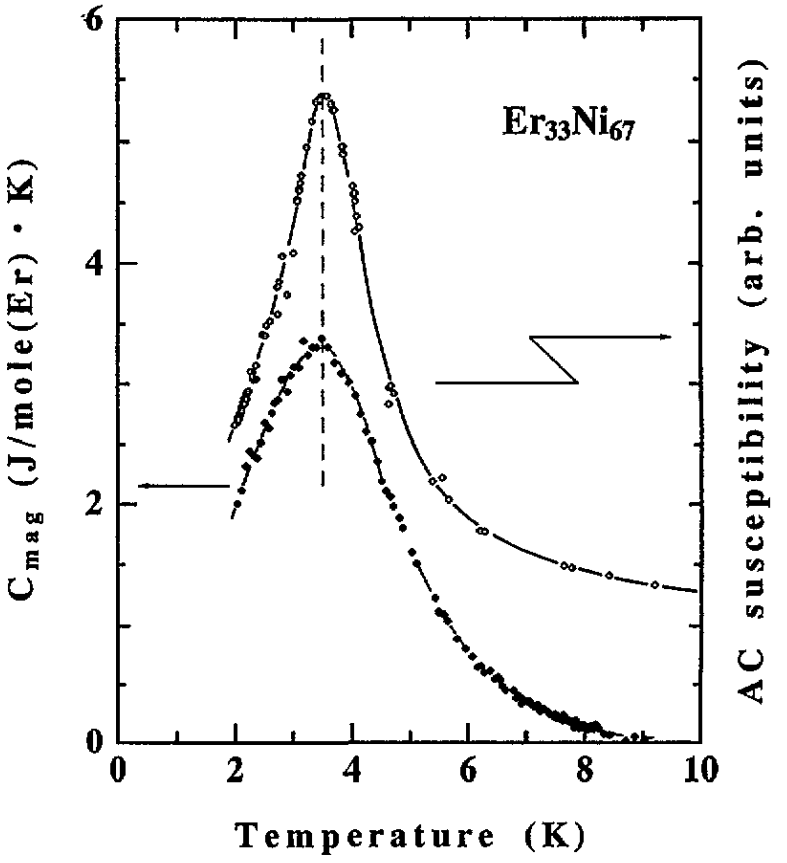

Figure 10. Temperature dependence of the magnetic contribution to the specific heat C_{mag} and that of the AC magnetic susceptibility of the amorphous $Er_{33}Ni_{67}$ alloy.

Figure 11 displays the temperature dependence of the magnetic entropy for the amorphous Er_xNi_{100-x} (x = 33 and 50) alloys. Experimentally, the magnetic entropy S_{mag} is given by

$$S_{mag}(T_M) = \int_0^{T_M} \frac{C_{mag}}{T} dT \tag{9}$$

where T_M is the long-range magnetic ordering temperature. The value of magnetic entropy S_{mag} for the amorphous $Er_{33}Ni_{67}$ and $Er_{50}Ni_{50}$ alloys obtained by integrating the C_{mag}/T versus T curves is closer to $R\ln 2$ rather than to $R\ln 16$ expected from the ground state $J = 15/2$ of the free Er^{3+} ion. Note that these results hardly depend on the estimation of θ_D because the lattice specific heat is very small at such low temperatures in the vicinity of T_f. These results indicate that the RMA splits the $J = 15/2$ ground state into Kramers doublets in a similar manner to the amorphous $Dy_{52}Cu_{48}$, $Dy_{54}Au_{46}$ and $Dy_{32}Ni_{68}$ alloys (von Molnar *et al* 1982). In the case of long-range magnetic transition, S_{mag} is nearly equal to the value of $R\ln(2J+1)$, where R is the gas constant and J the angular momentum quantum number. On the other hand, the S_{mag} at T_f for spin-glass systems such as crystalline magnetically dilute AuFe and CuMn alloys has been reported to be 22–33% of the theoretical values

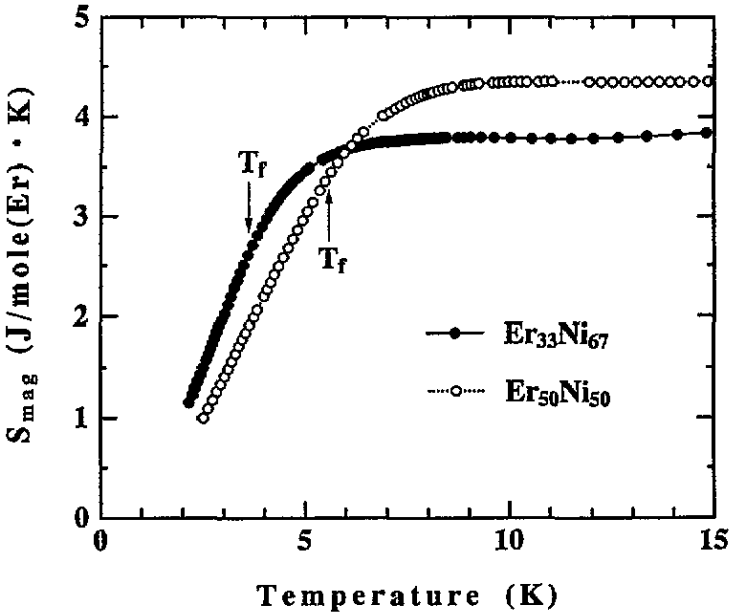

Figure 11. Temperature dependence of the magnetic entropy S_{mag} for the amorphous Er_xNi_{100-x} ($x = 33$ and 50) alloys. The arrows indicate the spin freezing temperature T_f.

$R\ln(2J+1)$ (Wenger and Keesom 1976). The magnitude of the magnetic entropy at T_f for the present amorphous $Er_{33}Ni_{67}$ and $Er_{50}Ni_{50}$ alloys is estimated to be about 45% and 60% of the theoretical value of $R\ln 2$, respectively, being much larger than that of the dilute AuFe and CuMn alloys mentioned above. In amorphous $Gd_{33}Al_{67}$ alloy, the magnetic entropy S_{mag} develops about 55% of the theoretical value, and this value lies between those of the ferromagnets and crystalline dilute spin-glass systems (Coey *et al* 1977). In addition, the magnetic specific heat of the amorphous $Gd_{33}Al_{67}$ alloy shows a $T^{3/2}$ temperature dependence, indicating a collective excitation (Coey *et al* 1977). These results indicate that ferromagnetic-like spin waves can be excited in the amorphous $Gd_{33}Al_{67}$ alloy, although the overall magnetic structure of this amorphous alloy is not ferromagnetic but spin-glass. Therefore, it is interesting to study the low-temperature specific heat characteristics for an alloy having the spin-glass-like behaviour induced by the RMA. Figure 12 displays the temperature dependence of the magnetic specific heat in the form of C_{mag} versus $T^{3/2}$ for the amorphous $Er_{50}Ni_{50}$ alloy. It is clear that the C_{mag} of this alloy follows the $T^{3/2}$ dependence up to about 4 K in a similar manner to that of the amorphous $Gd_{33}Al_{67}$ alloy. From the $T^{3/2}$ dependence of magnetic specific heat, the ferromagnetic-like spin wave would also be excited in the present amorphous Er–Ni alloys, resulting in the large development of S_{mag} at T_f and in the coincidence between the maximum temperature of the magnetic specific heat and T_f.

4. Summary

The competition between ferromagnetic and antiferromagnetic exchange interactions is very small and the magnetic ordering temperature is low in amorphous Er_xNi_{100-x} ($x = 33, 50$

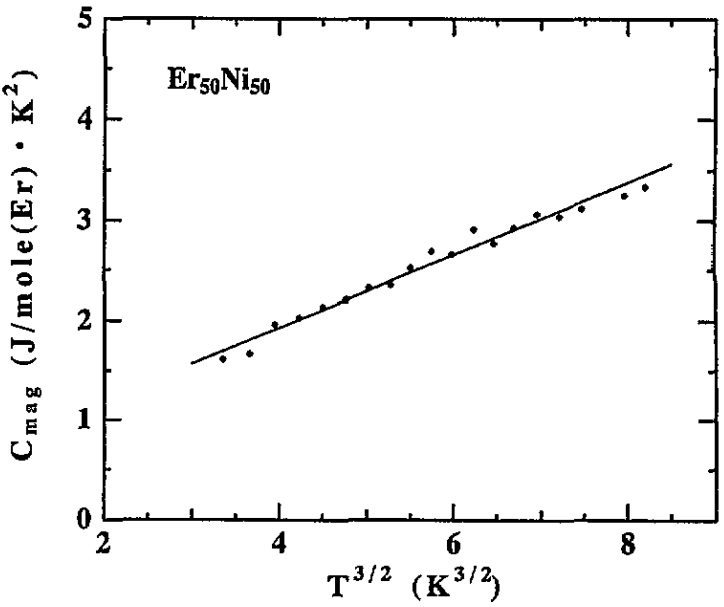

Figure 12. Temperature dependence of the magnetic contribution to the specific heat C_{mag} for the amorphous $Er_{50}Ni_{50}$ alloy in the form of C_{mag} versus $T^{3/2}$.

and 80) alloys. Therefore, this alloy system is appropriate to elucidate the effect of random magnetic anisotropy on low-temperature magnetic properties. In the present study, various magnetic properties and low-temperature specific heat have been investigated. The main results are summarized as follows:

(i) Because of the random magnetic anisotropy (RMA), the amorphous Er_xNi_{100-x} alloys exhibit spin-glass-like behaviour. The spin freezing temperature T_f increases with increasing Er content.

(ii) The random magnetic anisotropy constant D becomes larger with the increase in the Er content. The magnetization per Er atom becomes smaller with increasing Er content because of the increase in the RMA.

(iii) The low-temperature specific heat exhibits a broad maximum at T_f, which is different from other spin-glass systems such as crystalline magnetically dilute CuMn alloys and $Eu_xSr_{1-x}S$ ($x = 0.40$ and 0.54) compounds.

(iv) The amorphous Er_xNi_{100-x} ($x = 33$ and 50) alloys exhibit a large linear term of the Schottky-type specific heat because the ground state of $J = 15/2$ splits into Kramers doublets due to the RMA. The Debye temperature θ_D of the amorphous $Er_{33}Ni_{67}$ and $Er_{50}Ni_{50}$ alloys is about 200 K and 180 K, respectively.

(v) The magnetic entropy at the spin freezing temperature T_f is estimated to be 45–60% of the theoretical value, being much larger than those of the crystalline magnetically dilute spin-glass alloys.

(vi) The magnetic contribution to the specific heat C_{mag} of the amorphous $Er_{50}Ni_{50}$ alloy exhibits a $T^{3/2}$ dependence, suggesting the excitation of a ferromagnetic-like spin wave.

Acknowledgments

The authors would like to thank Dr T H Chiang for technical assistance in the experimental work. The support by a Grant-in-Aid for Development Scientific Research (B)(2), 05555178, from the Japanese Ministry of Education, Science and Culture, is appreciated.

References

Aharony A and Pytte E 1980 *Phys. Rev. Lett.* **45** 1583–6
Asomoza R, Campbell I A, Fert A, Lénard A and Rebouillat J P 1979 *J. Phys. F: Met. Phys.* **9** 349–71
Beille J, Liénard J R and Rebouillat J P 1979 *J. Physique Coll.* **40** C5 256–7
Boucher B 1977a *Phys. Status Solidi* a **40** 197–203
—— 1977b *IEEE Trans.* **MAG-13** 1601–2
Cannella V and Mydosh J A 1972 *Phys. Rev.* B **6** 4220–37
Coey J M D 1978 *J. Appl. Phys.* **49** 1646–52
Coey J M D, McGuire T R and Tissier B 1981 *Phys. Rev.* B **24** 1261
Coey J M D, von Molnar S and Gambino R J 1977 *Solid State Commun.* **24** 167–70
Coles B R, Jamieson H, Taylor R H and Tari A 1975 *J. Phys. F: Met. Phys.* **5** 565–74
de Almeida J R and Thouless D J 1978 *J. Phys. A: Math. Gen.* **11** 983–90
Filippi J, Dieny B and Barbara B 1985 *Solid State Commun.* **53** 523–7
Fujita A, Chiang T H, Kataoka N and Fukamichi K 1993 *J. Phys. Soc. Japan* **62** 2579–82
Gignoux D, Givord D and Liénard A 1982 *J. Appl. Phys.* **53** 2321–3
Harris R, Plischke M and Zuckermann M J 1973 *Phys. Rev. Lett.* **16** 160–2
Hattori Y, Takada Y, Fukamichi K, Katori A H and Goto T 1995 *J. Phys.: Condens. Matter* submitted
Jamet J P and Malozemoff A P 1978 *J. Appl. Phys.* **53** 2321–3
Korenblit I Ya and Shender E F 1978 *J. Phys. F: Met. Phys.* **8** L197–9
Liénard A and Rebouillat J P 1978 *J. Appl. Phys.* **49** 1680–2
McGuire T R, Mizoguchi T, Gambino R J and Kirkpatrick S 1978 *J. Appl. Phys.* **49** 1689–90
Meschede D, Steglich F, Felsch W, Maletta H and Zinn W 1980 *Phys. Rev. Lett.* **44** 102–5
Miyako Y, Sato T, Kimishima Y and Yuochunas Y G 1979 *J. Phys. Soc. Japan* **46** 1379–80
Mizoguchi T, McGuire T R, Gambino R J and Kirkpatrick S 1977 *Physica* **86–88B** 783–4
O'Shea M J and Lee K M 1991 *J. Magn. Magn. Mater.* **99** 103–18
Rebouillat J P, Liénard A, Coey J M D, Arrese-Boggiano R and Chappert J 1977 *Physica* **86–88B** 773–4
Sellmyer D J, Hadjipanayis G and Cornelison S G 1980 *J. Non-Cryst. Solids* **40** 437–45
Sellmyer D J and Nafis S 1985 *J. Appl. Phys.* **57** 3584–8
von Molnar S, McGuire T R and Gambino R J 1982 *J. Appl. Phys.* **53** 7666–71
Wenger L E and Keesom P H 1976 *Phys. Rev.* B **13** 4053–9